(2)

MTL TR 89-17

AD

SOLVENT ASSISTED DELAMINATION CRACK GROWTH BEHAVIOR OF AMORPHOUS THERMOPLASTIC MATERIALS

ALEX J. HSIEH and JANICE J. VANSELOW
POLYMER RESEARCH BRANCH

AD-A207 365

February 1989

US ARMY
LABORATORY COMMAND
MATERIALS TECHNOLOGY LABORATORY

Sponsored by
U.S. Army Chemical Research, Development and
Engineering Center, Aberdeen Proving Ground, MD

U.S. ARMY MATERIALS TECHNOLOGY LABORATORY
Watertown, Massachusetts 02172-0001

The findings in this report are not to be construed as an official Department of the Army position, unless so designated by other authorized documents.

Mention of any trade names or manufacturers in this report shall not be construed as advertising nor as an official indorsement or approval of such products or companies by the United States Government.

DISPOSITION INSTRUCTIONS

Destroy this report when it is no longer needed.
Do not return it to the originator.

UNCLASSIFIED

SECURITY CLASSIFICATION OF THIS PAGE (When Data Entered)

REPORT DOCUMENTATION PAGE		READ INSTRUCTIONS BEFORE COMPLETING FORM
1. REPORT NUMBER MTL TR 89-17	2. GOVT ACCESSION NO.	3. RECIPIENT'S CATALOG NUMBER
4. TITLE (and Subtitle) SOLVENT ASSISTED DELAMINATION CRACK GROWTH BEHAVIOR OF AMORPHOUS THERMOPLASTIC MATERIALS		5. TYPE OF REPORT & PERIOD COVERED Final Report 6. PERFORMING ORG. REPORT NUMBER
7. AUTHOR(s) Alex J. Hsieh and Janice J. Vanselow		8. CONTRACT OR GRANT NUMBER(s)
9. PERFORMING ORGANIZATION NAME AND ADDRESS U.S. Army Materials Technology Laboratory Watertown, Massachusetts 02172-0001 SLCMT-EMP		10. PROGRAM ELEMENT, PROJECT, TASK AREA & WORK UNIT NUMBERS AMCMS Code: 612105.H840011 Agency Accession: 2182040
11. CONTROLLING OFFICE NAME AND ADDRESS U.S. Army Chemical Research, Development and Engineering Center Aberdeen Proving Ground, Maryland 21010-5423		12. REPORT DATE February 1989 13. NUMBER OF PAGES 14
14. MONITORING AGENCY NAME & ADDRESS(if different from Controlling Office)		15. SECURITY CLASS. (of this report) Unclassified 15a. DECLASSIFICATION/DOWNGRADING SCHEDULE

16. DISTRIBUTION STATEMENT (of this Report)

Approved for public release; distribution unlimited.

17. DISTRIBUTION STATEMENT (of the abstract entered in Block 20, if different from Report)

18. SUPPLEMENTARY NOTES

Presented at CRDEC Conference on Chemical Defense Research, Aberdeen Proving Ground, November 15-18, 1988.

19. KEY WORDS (Continue on reverse side if necessary and identify by block number)

Environmental tests	Polyetherimide	Fracture mechanics
Amorphous materials	Thermoplastic	Adhesives
Composite materials	Residual stress	Toughness
Delamination	Crack propagation	Mosaic cracks

20. ABSTRACT (Continue on reverse side if necessary and identify by block number)

(SEE REVERSE SIDE)

DD FORM 1 JAN 73 1473 EDITION OF 1 NOV 65 IS OBSOLETE

UNCLASSIFIED

SECURITY CLASSIFICATION OF THIS PAGE (When Data Entered)

Block No. 20

ABSTRACT

Crack growth studies are being carried out with o-xylene in an amorphous thermoplastic, polyetherimide (PEI), via a static deadweight loading apparatus. The three systems evaluated were the neat resin, composite, and adhesively bonded composite. The neat resin specimens show striationlike crack growth band markings on the fracture surfaces. The spacing between the growth bands increases with increasing crack length in each specimen. In the case of the adhesively bonded composite, a characteristic mosaic pattern of intersecting cracks normal to the plane of the adhesive was seen on the fracture surfaces. These cracks, as well as matrix cracks perpendicular to the fibers seen on the fractured composite specimens, appear to result from residual stress driven solvent cracking. Although the rates of crack propagation in the composite systems are much slower than those in the neat resin at most G_I values, the mode of solvent-induced degradation is shown to be matrix dominated.

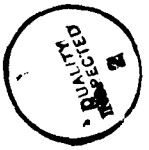

INTRODUCTION

There has been a large growth in the use of polymeric composites in military applications. The replacement of traditional materials, primarily metals, with composite structure is favored in order to reduce the weight of components, and improve fuel efficiency, as well as to achieve higher specific modulus and specific strength. Fiber-reinforced composite structures usually consist of many layers or laminae stacked up in a predetermined arrangement to attain optimum properties and performance. However, composite materials have low interlaminar strengths compared to their strengths parallel to the fiber, which can result in delamination.

Currently, the matrices chosen in most systems have had thermoset characteristics, such as high cross-link density, high stiffness, and brittleness. The resistance to interlaminar crack propagation has been known to be dominated by the fracture toughness of the neat resins;[1,2] therefore, the low fracture toughness of the brittle matrix usually translates into poor composite interlaminar strength. Considerable concern over delamination-induced fracture has brought a number of research groups to investigate the use of tougher matrix materials.[2]

Despite their toughness, some of the thermoplastics are susceptible to the attack of many organic solvents while under stress, including CW agents and decontaminates. The stress can either be mechanically induced or a residual thermal stress due to thermal coefficient of expansion mismatches and high processing temperatures. Such solvent-enhanced degradation can cause problems in the service environments as seen in many amorphous glassy polymers.[3]

Understanding the fundamental failure mechanisms of solvent-enhanced stress cracking is of practical importance in order to improve the durability of the advanced composites. In the present paper, o-xylene is selected as a cracking agent to study the crack growth of an amorphous polyetherimide as in the neat resin, composite, and adhesively bonded composite systems.

EXPERIMENTAL METHODS

The double cantilever beam (DCB) specimen, shown in Figure 1, was used to study Mode I delamination crack growth in the composites. A Teflon-coated glass fabric was inserted between the center plies at one end during lay-up. This was to provide a starter notch for subsequent crack propagation. The compact tension (CT) specimen per ASTM E 399,[4] in Figure 2, was used to study crack propagation in the neat resin. These test specimens were subjected to droplets of o-xylene while under a constant load. The crack length measurements were made as a function of time with either a traveling microscope or a camera.

1. BRADLEY, W. L., and COHEN, R. N. *Matrix Deformation and Fracture in Graphite-Reinforced Epoxies.* ASTM STP 876, 1985, p. 389.
2. HUNSTON, D. L., MOULTON, R. J., JOHNSTON, N. J., and BASCOM, W. D. *Matrix Resin Effects in Composite Delamination: Mode I Fracture Aspects.* ASTM STP 937, 1987, p. 74.
3. KAMBOUR, R. P. *A Review of Crazing and Fracture in Thermoplastics.* General Electric Report No. 72CRD285, October 1972.
4. *Standard Method of Test for Plane-Strain Fracture Toughness of Metallic Materials.* 1988 Annual Book of ASTM Standards, Technical Report Designation E 399-83, 1983, p. 681.

The parameter which measures the resistance to crack propagation is called the stress intensity factor K_I or the associated strain energy release rate, G_I. ASTM compact tension test yields stress intensity factor, K_I, via Equation 1, from which G_I of the neat resin can be calculated via Equation 2.

$$K_I = P/(Bw^{1/2})[29.6(a/w))^{1/2} - 185.5(a/w)^{3/2} + 655.7(a/w)^{5/2} - 1017(a/w)^{7/2} + 638.7(a/w)^{9/2}] \quad (1)$$

and

$$G_I = \frac{K_I^2}{E} (1 - \nu^2) \quad (2)$$

where K_I = stress intensity factor
P = load
B = specimen thickness
w = specimen width
a = crack length
E = Young's modulus
ν = Poisson's ratio.

Using the compliance method,[5] G_I for composite DCB specimen can be calculated as

$$G_I = \frac{P^2}{2w} \frac{dC}{da} \quad (3)$$

and

$$C = \delta / P \quad (4)$$

where C is the compliance, and δ is the displacement of the crack ends at any crack length.

RESULTS AND DISCUSSION

Stress versus lifetime measurements have been used in many environment stress cracking studies. Although such tests are still useful, it is recognized that fracture mechanics based tests can provide better understanding of the basic mechanisms involved. In this work, precracked specimens for both neat resin and composite are such that a constant deadweight load results in increasing strain energy release rate with increasing crack length.

Figure 3 shows the neat resin raw data for the crack length versus time as a function of initial load. These data, after being reduced in terms of G_I, are superimposable as shown in Figure 4. However, G_I values in solvent-assisted stress cracking are significantly lower than the critical value needed for the neat resin (G_{IC} = 3.2 kJ/m^2) to grow a crack in air.

Scanning electron microscopy (SEM) studies were carried out on the fracture surfaces of the test specimens. In addition to a flat glassy appearance compared to those tested in air, the neat resin specimens tested in o-xylene show striationlike crack growth band markings on the fracture surface, as seen in Figure 5, which trace out crack front positions at particular values of time. The spacing between the

5. RUSSELL, A. J., and STREET, K. N. *Moisture and Temperature Effects on the Mix-Mode Dclamination Fracture of Unidirectional Graphite/Epoxy.* ASTM STP 876, 1985, p. 349.

growth bands increases with increasing crack length in each specimen. In Figure 6, at 1000X magnification, discontinuous growth bands are clearly seen, which are similar to those under fatigue crack growth in air for many glassy amorphous polymers.[6,7] At a higher magnification (2000X), a distinct morphology of "patch" patterns are seen in Figure 7, reflecting the craze matter just before crack propagation, which decrease in size in the direction of crack growth.

Figure 8 shows that the crack growth rates in the composite are much slower than in the neat resin at most G_I values. Multiple cracking on the adjacent layers, as well as ahead of the main crack tip, was noticed on the profile of the tested composite specimen. In addition, matrix cracks perpendicular to the fiber direction within the weave are shown in Figures 9 and 10. This solvent-assisted stress cracking is attributed to the presence of residual thermal stress between the fibers and their surrounding matrix, resulting from the cool-down process.

The importance of the residual stress driven stress cracks was further addressed in the studies of adhesively bonded composites. The approach taken was to prepare test specimens, in which solvent-sensitive adhesive was built into the solvent-resistant composite. The specimens were fabricated from prepreg with PEI film adhesive between the center plies, and in various thicknesses. The matrix in the prepreg is a newly developed PEI resin with good resistance to o-xylene, which has a different PEI formulation than that in the neat resin and in the film adhesive.

In the adhesively bonded PEI composites, the delamination crack growth rates are shown in Figure 11 to increase with the thickness of the adhesive layer.[8] Figure 12 compares the neat resin data with data for the adhesively bonded composites. Results show that the rates of crack propagation in the adhesive systems are much slower than in the neat resin. Figures 13 to 15 of the fracture surfaces show a characteristic mosaic fracture pattern. The thicker the adhesive layer, the larger the size of mosaic cracks. This indicates that the residual biaxial tensile stress field is sufficient to drive the solvent-assisted cracks throughout the adhesive region prior to the growth of the main crack. While the bidirectional crack pattern propagates through the adhesive layer, it draws in more and more solvent to feed further expansion of the crack system. When the main crack finally passes, it must continually reinitiate failures in the individual blocks of the remaining adhesive, which are still well-bonded to the laminate.

For the 2-mil-thick specimen, the rate of crack growth is much slower than for the others. This has been attributed to the effect of the fabric weave, which tends to press the adhesive layer to a very thin condition at the weave crossover points. Consequently, the fibers appear to interfere with crack growth, while the crack grows faster in the resin-rich zones between these points. The weave effect is evident in Figure 15.

In the case of a thick adhesive, the nucleation points and crack growth band markings within each block are seen in Figure 16; thinner adhesives show some propagation from block to block (Figure 17). Smaller band spacings, seen in the adhesively bonded composites compared to those in the neat resins, indicate that crack reinitiation occurs at lower G_I level within each mosaic block.

6. DOLL, W. *Optical Interference Measurements and Fracture Mechanics Analysis of Crack Tip Craze Zones* in Advances in Polymer Science, Springer-Verlag, Berlin Heidelberg, v. 52/53, 1983, p. 153.
7. HERTZBERG, R. W., and MANSON, J. A. *Fatigue of Engineering Plastics.* Academic Press, New York, 1980, p. 160-169.
8. HSIEH, A. J., and MANDELL, J. F. *Environment Enhanced Delamination Crack Growth of Adhesively Bonded Polyetherimide Matrix Composite.* Proceedings of the ACS Division of Polymeric Materials: Sci. and Eng., v. 59, 1988, p. 945.

CONCLUSIONS

The mode of solvent-assisted stress cracking in the neat resin, composite, and adhesively bonded composite is shown to be matrix dominated. The residual thermal stress is sufficiently high to drive solvent stress cracks in the matrix, as well as in the adhesive layer. In the case of adhesively bonded composites, the size of mosaic cracks increases as the adhesive layer thickness increases, as does the rate of delamination crack growth. The need to reinitiate a crack within each mosaic block greatly retards the main crack growth; consequently, the crack growth rates are much slower than those in the neat resin at most G_I values. Finally, it is not overemphasized that solvent stress cracking can be very important not only for glassy polymers, but also for composites with amorphous thermoplastic matrices.

ACKNOWLEDGMENT

The authors wish to thank Professor John F. Mandell of Montana State University for very helpful discussions throughout this work.

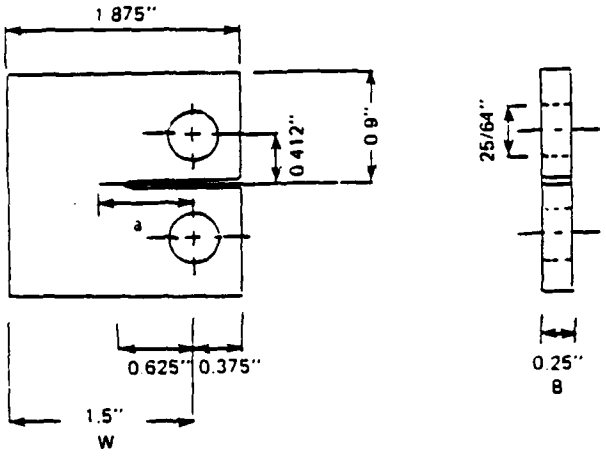

Figure 1. Compact tension (CT) specimen geometry per ASTM E 399-83.

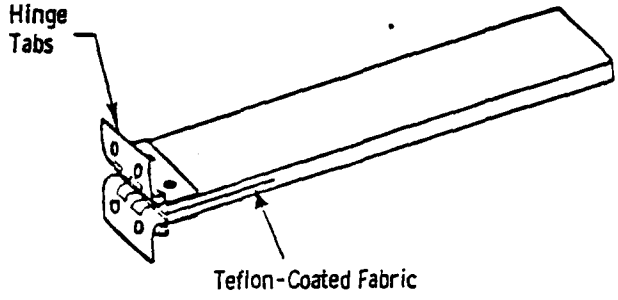

Figure 2. Sketch of double cantilever beam (DCB) specimen.

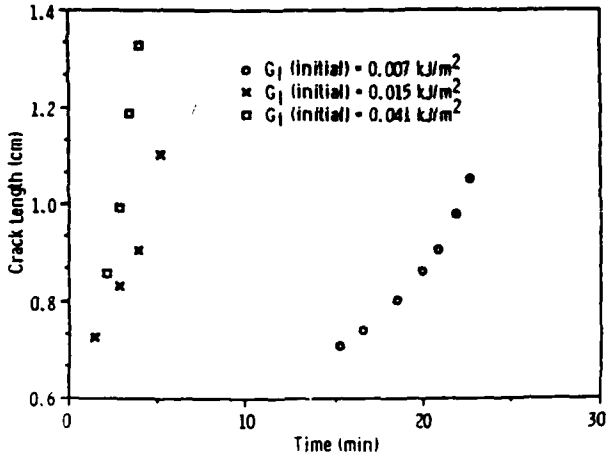

Figure 3. Crack length versus time as a function of initial G_I in the neat resin CT specimens.

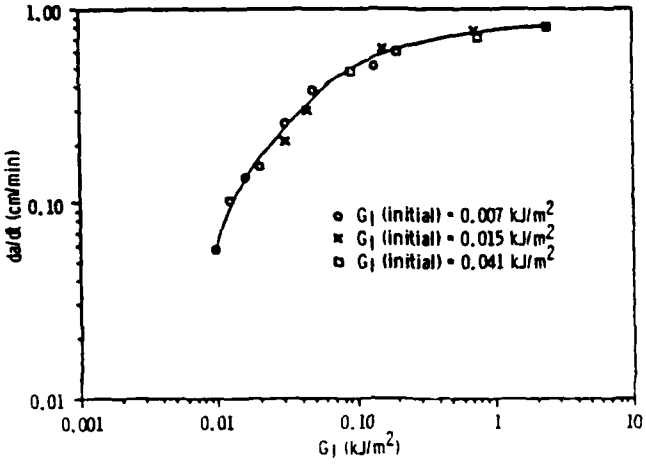

Figure 4. Crack growth rate versus G_I for the data in Figure 3.

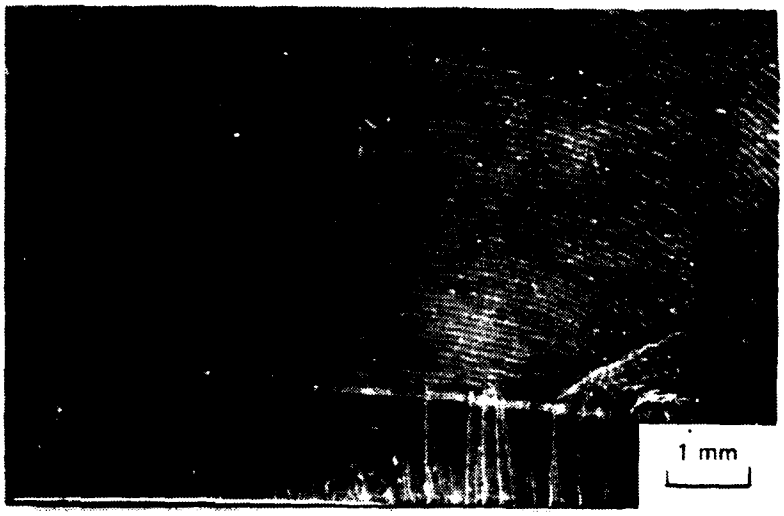

Figure 5. SEM micrograph shows crack growth band markings on the neat resin fracture surface.

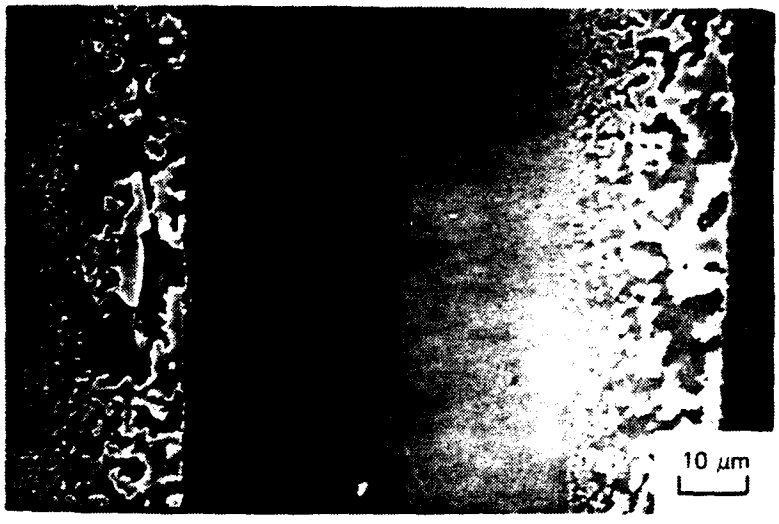

Figure 6. SEM micrograph clearly shows discontinuous growth bands on the neat resin fracture surface.

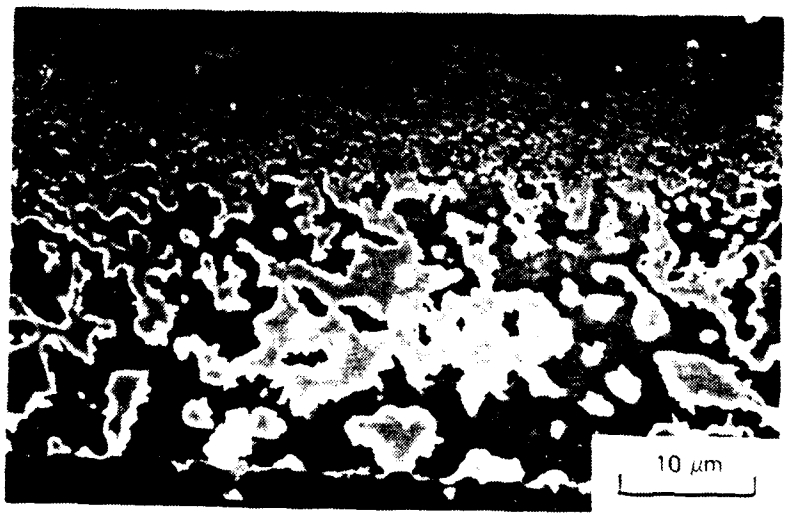

Figure 7. SEM micrograph shows the size of "patch" pattern decreases in the direction of crack growth.

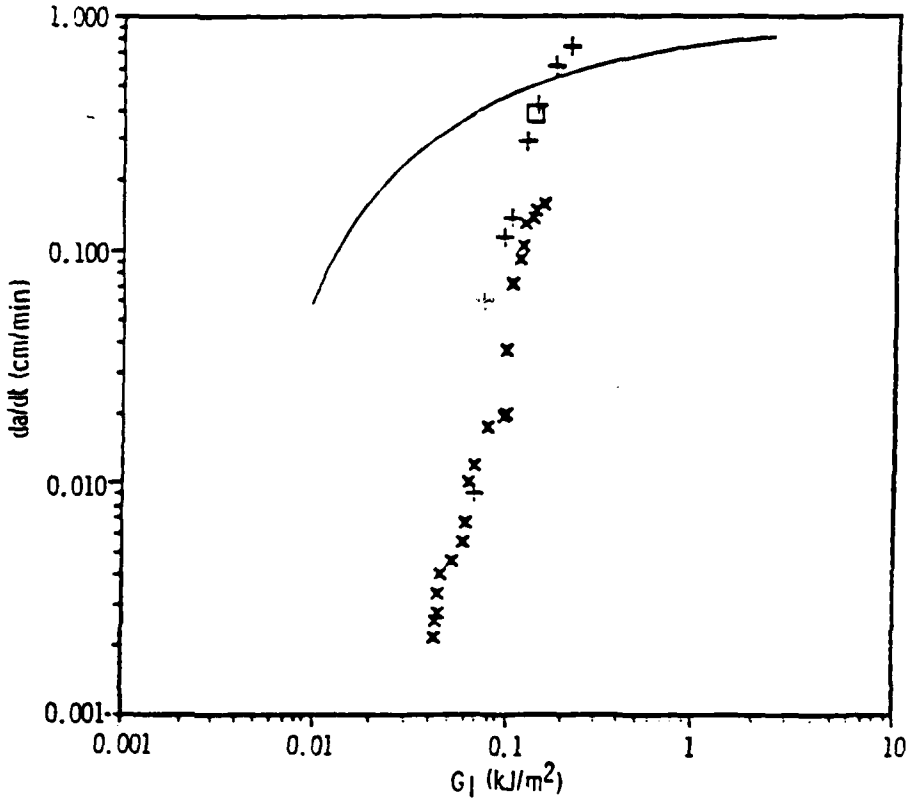

Figure 8. Comparison of the composite data with the data for the neat resin (solid line is for neat resin as in Figure 4).

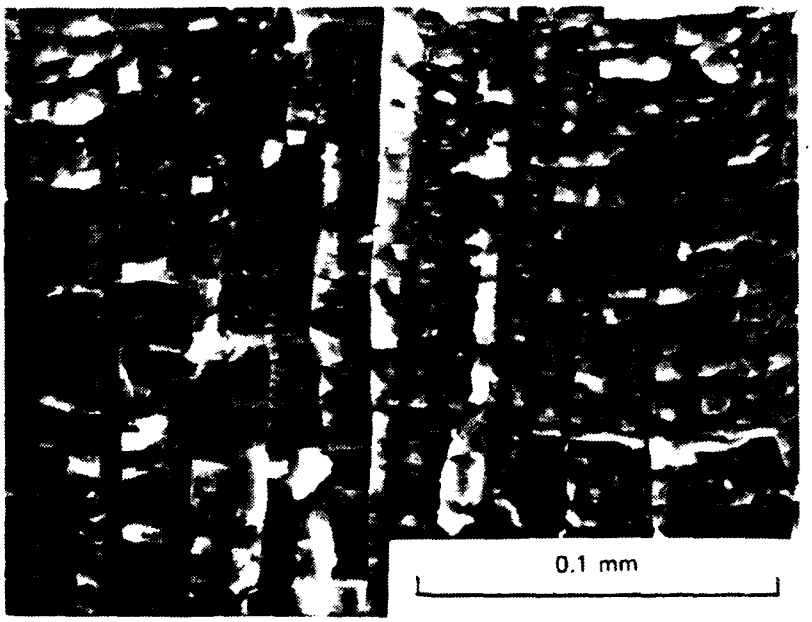

Figure 9. SEM micrograph shows matrix cracks perpendicular to the fibers on the fractured composite specimen.

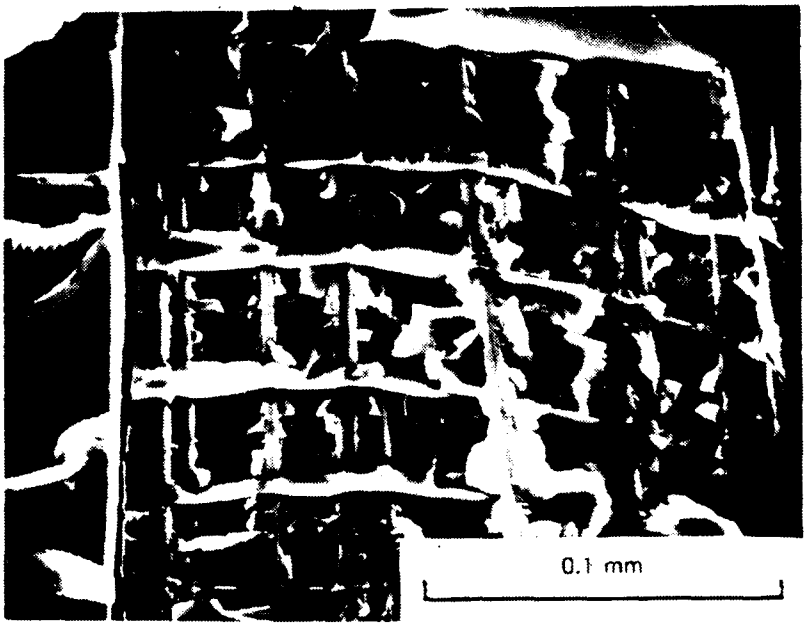

Figure 10. SEM micrograph shows matrix cracks perpendicular to the fibers on the fractured composite specimen.

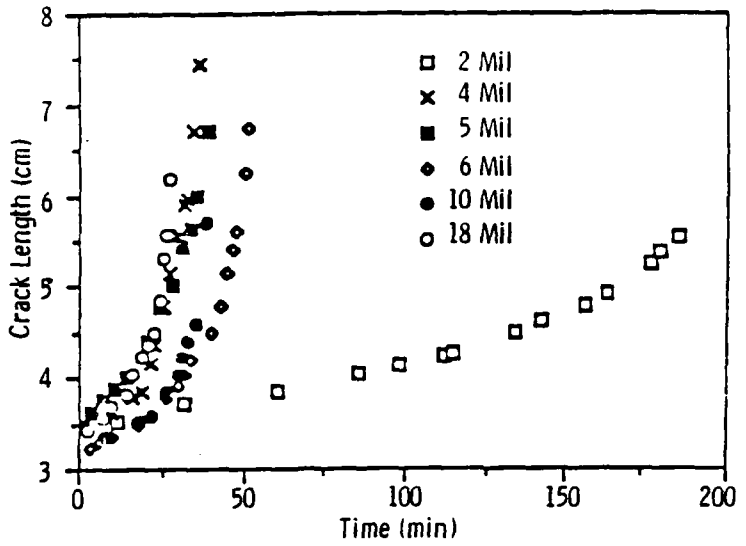

Figure 11. Crack length versus time for various adhesive thicknesses at the same force level.

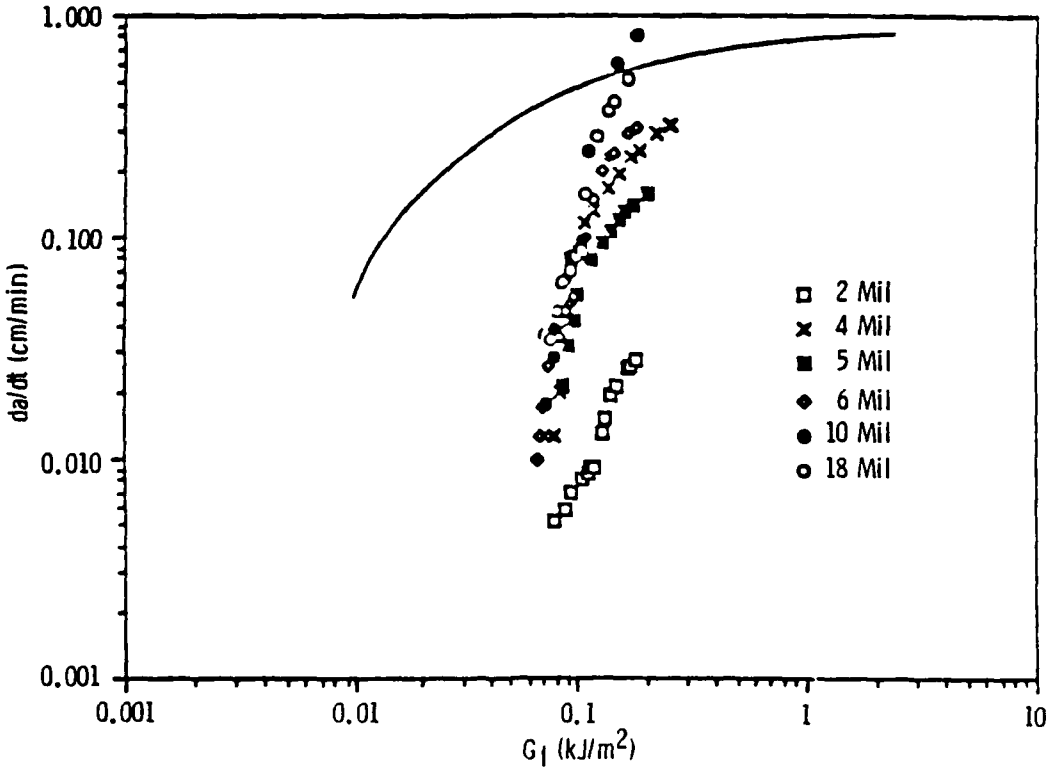

Figure 12. Comparison of the neat resin data (solid line from Figure 4) with the data for the adhesively bonded composites.

Figure 13. SEM micrograph shows a characteristic mosaic crack pattern on the fracture surface of the composite specimen with 18-mil-thick PEI film adhesive.

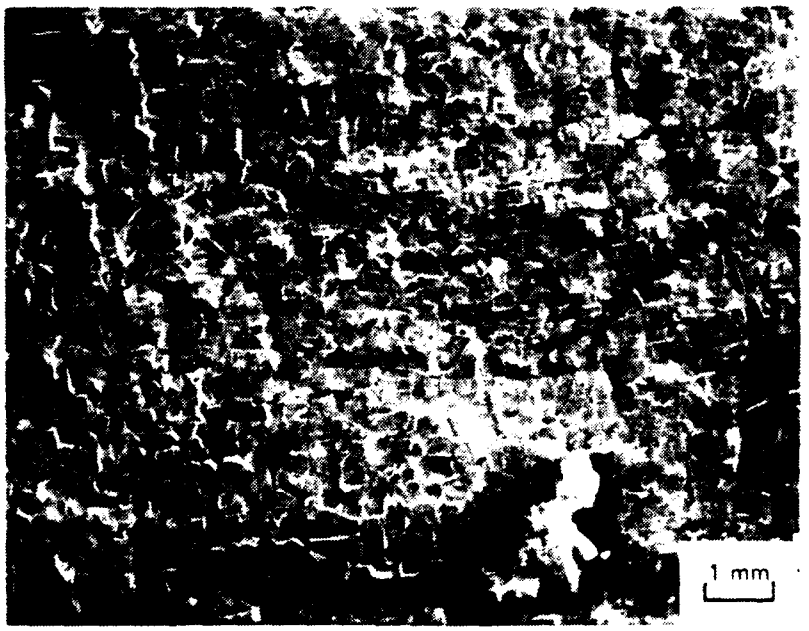

Figure 14. SEM micrograph shows a characteristic mosaic crack pattern on the fracture surface of the composite specimen with 6-mil-thick PEI film adhesive.

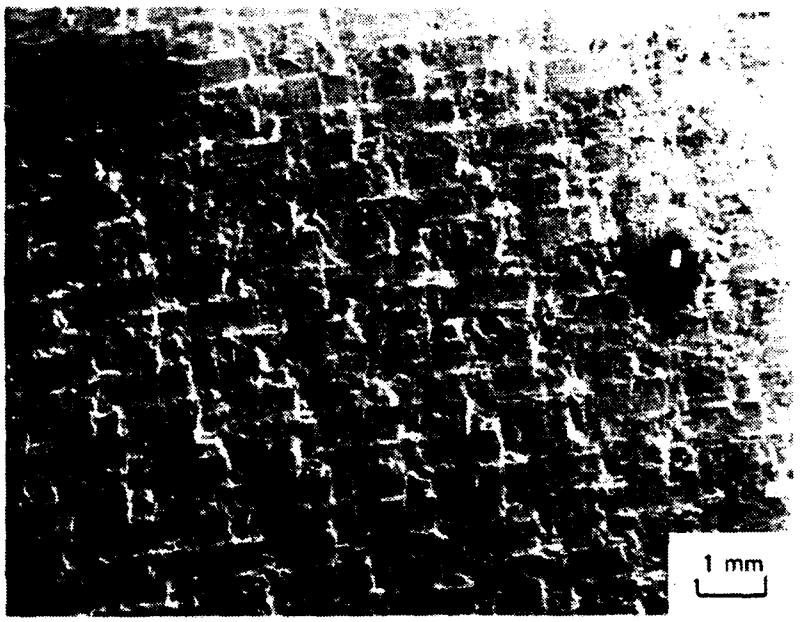

Figure 15. SEM micrograph of the fracture surface of the composite specimen with 2-mil-thick PEI film adhesive.

Figure 16. SEM micrograph shows nucleation point and growth band markings on the composite fracture surface.

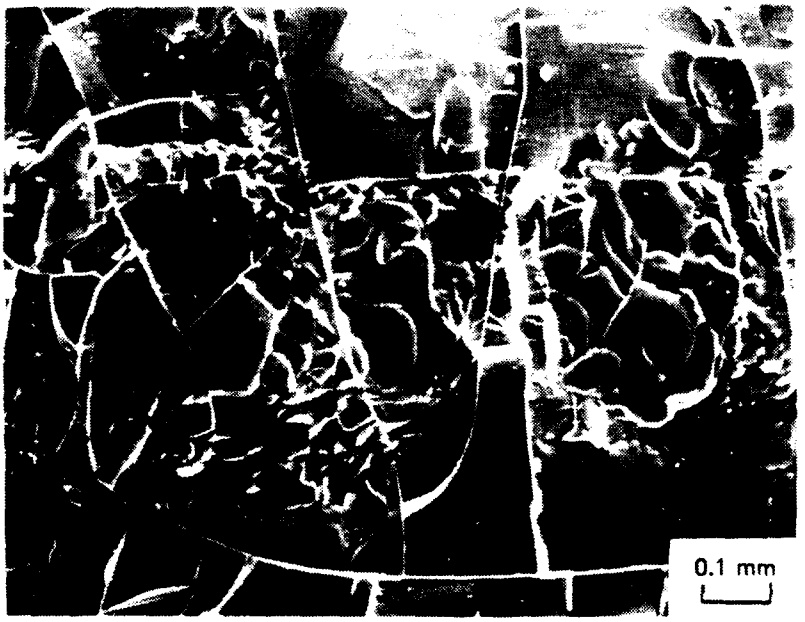

Figure 17. SEM micrograph shows crack propagation from block-to-block for the composite specimen with 4-mil-thick PEI film adhesive.

DISTRIBUTION LIST

No. of Copies	To
	Commander, U.S. Army Chemical Research, Development and Engineering Center, Aberdeen Proving Ground, MD 21010-5423
1	ATTN: SMCCR-ODE
1	SMCCR-ODD
1	SMCCR-ODP
1	SMCCR-HV
1	SMCCR-MSI
1	SMCCR-MU
1	SMCCR-MUC
1	SMCCR-MUP
1	SMCCR-NB
1	SMCCR-OPC (B. Eckstein)
1	SMCCR-OPF
1	SMCCR-OPP
1	SMCCR-OPR
1	SMCCR-PPC
1	SMCCR-PPI
1	SMCCR-PPP
1	SMCCR-RS
2	SMCCR-RSC (E. Penski, W. Shuely)
1	SMCCR-RSL
1	SMCCR-RSP
1	SMCCR-RSP-A (M. Miller)
1	SMCCR-RSP-B
1	SMCCR-RSP-P
1	SMCCR-RST
1	SMCCR-SF
1	SMCCR-SPS-T
1	SMCCR-ST
1	SMCCR-TDT (S. Lawhorne)
1	SMCCR-MUA (Record copy)
	Commandant, U.S. Army Ordnance Missile and Munitions Center and School, Redstone Arsenal, AL 35897-6700
1	ATTN: ATSK-EI (Mr. Cranford)
	Commander, U.S. Army Missile Command, Redstone Scientific Information Center, Redstone Arsenal, AL 35898-5241
1	ATTN: AMSMI-RD-CS-R (Document Section)
	Commander, U.S. Army Missile Command, Redstone Arsenal, AL 35898-5241
1	ATTN: AMSMI-ROC (Dr. B. Fowler)
	Commander, U.S. Army Missile Command, Redstone Arsenal, AL 35898-5500
1	ATTN: AMSMI-RGT (Mr. Maddix)
1	AMSMI-YDL, Bldg. 4505
1	AMSMI-YLP (Mr. N. C. Kattos)
	Commander, Anniston Army Depot, Anniston, AL 36201-5009
1	ATTN: SDSAN-CS
	Commandant, U.S. Army Chemical School, Fort McClellan, AL 36205-5020
1	ATTN: ATZN-CM
1	ATZN-CM-CC
1	ATZN-CM-CS
1	ATZN-CM-CT
1	ATZN-CM-MLB
1	ATZN-CM-NC
	Commander, U.S. Army Aviation Center, Fort Rucker, AL 36362-5000
1	ATTN: ATZQ-CAT-CA-M (CPT P. McCluskey)
1	ATZQ-D-MS
	Commander, U.S. Army Electronic Proving Ground, Fort Huachuca, AZ 85613-7110
1	ATTN: STEEP-DT-F
	Commander, Naval Weapons Center, China Lake, CA 93555
1	ATTN: Code 36
1	Code 366
1	Code 3554
1	Code 3653
1	Code 3656
1	Code 3664
1	Code 3893 (Dr. L. A. Matthews)
1	Code 3917 (Mr. D. V. Houwen) NWC Coordinator
	Commander, U.S. Army Science and Technology Center, Far East Office, San Francisco, CA 96328-5000
1	ATTN: Medical/Chemical Officer
1	AFOPRC/PR, Lowry Air Force Base, CO 80230-5000
1	NORAD/NC CBN, Cheyenne Mountain AFS-STOP 1, Peterson Air Force Base, CO 80914-5601

No. of Copies	To
	Director, Office of Environmental and Life Sciences, Office of the Under Secretary of Defense (R&E), The Pentagon, Washington, DC 20301-3080
1	ATTN: Mr. Thomas R. Oashiell
	Director, Defense Intelligence Agency, Washington, DC 20301-6111
1	ATTN: DT-5A (Mr. C. Clark)
1	HQDA (DAMO-NCC), Washington, DC 20310-0403
1	HQDA (DAMI-FIT-S&T), Washington, DC 20310-1087
1	HQ USAF/INKL, Washington, DC 20330-1550
1	HA AFOSR/NE, Bolling Air Force Base, Washington, DC 20332-6448
	Commander, Naval Air Systems Command, Washington, DC 20361
1	ATTN: PMA 279A (B. Motsuk)
1	PMA 279C (LCDR F. Smartt)
	Commander, Naval Sea Systems Command, Washington, DC 20362-5101
1	ATTN: Code 55X25
	Commander, Naval Sea Systems Command, Theater of Nuclear Warfare Program Office, Washington, DC 20362-5101
1	ATTN: Code TN20A (Dr. G. Patton)
	Commander, Naval Medical Command, Washington, DC 20372-5120
1	ATTN: MEDCOM-02C
	Commander, Naval Research Laboratory, 4555 Overlook Avenue, SW, Washington, DC 20375-5000
1	ATTN: Code 2526 (Library)
1	Code 6182 (Dr. R. Taylor)
	Commanding Officer, Navy Intelligence Support Center, Washington, DC 20390
1	ATTN: NISC-633 (Collateral Library)
	Commanding General, Marine Corps Research, Development and Acquisition Command, Washington, DC 20380-0001
1	ATTN: Code SSC NBC
1	Toxicology Information Center, JH, 652, National Research Council, 2101 Constitution Avenue, NW, Washington, DC 20418
	Director, Central Intelligence Agency, Washington, DC 20505
1	ATTN: AMR/ORD/DD/S&T
1	OSU Field Office, P.O. Box 1925, Eglin Air Force Base, FL 32542-1925
	Headquarters, Eglin Air Force Base, FL 32542-6008
1	ATTN: AD/YQO/YQX
1	USAFTAWC/THLO
1	AD/YN
1	Mr. L. Rodgers
	Commandant, U.S. Army Infantry School, Fort Benning, GA 31905-5410
1	ATTN: ATSH-CD-CS-CS
	Commander, U.S. Army Infantry Center, Fort Benning, GA 31905-5273
1	ATTN: NBC Branch, Directorate of Plans and Training, Bldg. 2294
	Commandant, U.S. Army Infantry School, Fort Benning, GA 31905-5410
1	ATTN: ATSH-B, NBC Branch
	Commandant, U.S. Army Infantry School, Fort Benning, GA 31905-5800
1	ATTN: ATSH-CD-MLS-C
	Commander, U.S. Army Armament, Munitions and Chemical Command, Rock Island, IL 61299-6000
1	ATTN: AMSMC-ASN
1	AMSMC-IMP-L
1	AMSMC-IRA
1	AMSMC-IRD-T
1	AMSMC-SF

No. of Copies	To
	Director, U.S. Army Materiel Command Field Safety Activity, Charlestown, IN 47111-9669
1	ATTN: AMXOS-SE (Mr. W. P. Yutmeyer)
	Commander, Naval Weapons Support Center, Crane, IN 47522-5050
1	ATTN: Code 5063 (Dr. J.R. Kennedy)
	Commander, U.S. Army TRADOC Independent Evaluation Directorate, Fort Leavenworth, KS 66027-5130
1	ATTN: ATZL-TIE-C (Mr. C. Annett)
	Commander, U.S. Army Combined Arms Center, Development Activity, Fort Leavenworth, KS 66027-5300
1	ATTN: ATZL-CAM-M
	Commander, U.S. Army Armor School, Fort Knox, KY 40121-5211
1	ATTN: ATZK-DPT (NBC School)
	Commander, U.S. Army Natick Research, Development, and Engineering Center, Natick, MA 01760-5015
1	ATTN: STRNC-AC
1	STRNC-UE
1	STRNC-WTS
1	STRNC-WT
1	STRNC-IC
1	STRNC-ICC
1	STRNC-IP
1	STRNC-ITP (Mr. Tassinari)
1	STRNC-YB
1	STRNC-YE
1	STRNC-YM
1	STRNC-YS
	Headquarters, Andrews Air Force Base, MD 20334-5000
1	ATTN: AFSC/SDTS
1	AFSC/SGB
	Commanding Officer, Naval Explosive Ordnance Disposal Technology Center, Indian Head, MD 20640-5070
1	ATTN: Code BC-2
1	Commander, Detachment S, USAOG, Team III, Fort Meade, MD 20755-5985
	Commander, Harry Diamond Laboratories, 2800 Powder Mill Road, Adelphi, MD 20783-1145
1	ATTN: DELHD-RT-CB (Dr. Sztankay)
	Commander, U.S. Army Laboratory Command, 2800 Powder Mill Road, Adelphi, MD 20783-1145
2	ATTN: Technical Library
	Director, U.S. Army Concepts Analysis Agency, 8120 Woodmont Avenue, Bethesda, MD 20814-2797
1	ATTN: CSCA-RQL (Dr. Helmbold)
	Director, U.S. Army Human Engineering Laboratory, Aberdeen Proving Ground, MD 21005-5001
1	ATTN: AMXHE-IS (Mr. Harrah)
	Project Manager, Smoke/Obscurants, Aberdeen Proving Ground, MD 21005-5001
2	ATTN: AMCPM-SMK-E (A. Van de Wal)
1	AMCPM-SMK-T
	Commander, U.S. Army Test and Evaluation Command, Aberdeen Proving Ground, MD 21005-5055
1	ATTN: AMSTE-TE-F
1	AMSTE-TE-T
	Director, U.S. Army Ballistic Research Laboratory, Aberdeen Proving Ground, MD 21005-5066
1	ATTN: SLCBR-OD-ST (Tech Reports)
	Director, U.S. Army Materiel Systems Analysis Activity, Aberdeen Proving Ground, MD 21005-5071
1	ATTN: AMXSY-CR (Mrs. F. Liu)
1	AMXSY-GC (Mr. F. Campbell)
1	AMXSY-MP (Mr. H. Cohen)
	Commander, U.S. Army Toxic and Hazardous Materials Agency, Aberdeen Proving Ground, MD 21010-5401
1	ATTN: AMXTH-ES
1	AMXTH-TE
	Commander, U.S. Army Environmental Hygiene Agency, Aberdeen Proving Ground, MD 21010-5422
1	ATTN: HSHB-O/Editorial Office

No. of Copies	To
	Commander, U.S. Army Armament, Munitions and Chemical Command, Aberdeen Proving Ground, MD 21010-5423
1	ATTN: AMSMC-HQ (A) (Mr. J. K. Smart)
1	AMSMC-QAC (A)
1	AMSMC-QAE (A)
	Commander, U.S. Army Technical Escort Unit, Aberdeen Proving Ground, MD 21010-5423
1	ATTN: AMCTE-AD
	Commander, U.S. Army Medical Research Institute of Chemical Defense, Aberdeen Proving Ground, MD 21010-5425
1	ATTN: SGRD-UV-L
	Director, Armed Forces Medical Intelligence Center, Building 1607, Fort Detrick, Frederick, MD 21701-5004
1	ATTN: AFMIC-IS
	Commander, U.S. Army Medical Bioengineering Research and Development Laboratory, Fort Detrick, Frederick, MD 21701-5010
1	ATTN: SGRB-UBG (Mr. Eaton)
1	SGRS-UBG-AL, Bldg. 568
	Commander, HQ 1/163d ACR, MT ARNG, P.O. Box 1336, Billings, MT 59103-1336
1	ATTN: NBC (SFC W. G. Payne)
	Director, U.S. Army Research Office, P.O. Box 12211, Research Triangle Park, NC 27709-2211
1	ATTN: SLCRO-CB (Dr. R. Ghirardelli)
1	SLCRO-GS
	Commander, U.S. Army Cold Regions Research and Engineering Laboratory, Hanover, NH 03755-1290
1	ATTN: CRREL-RG
	Commander, U.S. Army Production Base Modernization Activity Dover, NJ 07801
1	ATTN: AMSMC-PBE-C(D)/Regber
	Commander, U.S. Army Armament, Research, Development, and Engineering Center, Picatinny Arsenal, NJ 07806-5000
1	ATTN: SMCAR-A-E (S. Morrow)
1	SMCAR-AE (R. A. Trifiletti)
1	SMCAR-CCT
1	SMCAR-FSF-B
1	SMCAR-MSI
1	SMCAR-AET (Bldg. 335)
	Project Manager, Cannon Artillery Weapons Systems, Picatinny Arsenal, NJ 07806-5000
1	ATTN: AMCPM-CAWS-A
	Director, Los Alamos National Laboratory, Los Alamos, NM 87545
1	ATTN: T-DOT MS P371 (S. Gerstl)
	Commander/Director, U.S. Army Atmospheric Sciences Laboratory, White Sands Missile Range, NM 88002-5501
1	ATTN: SLCAS-AE (Dr. F. Niles)
1	SLCAS-AE-E (Dr. D. Snider)
1	SLCAS-AR (Dr. E. H. Holt)
1	SLCAS-AR-A (Dr. M. Heaps)
1	SLCAR-AR-P (Dr. C. Bruce)
1	SLCAR-AR-M (Dr. R. Sutherland)
	Director, U.S. Army TRADOC Analysis Command, White Sands Missile Range, NM 88002-5502
1	ATTN: ATOR-TSL
1	ATOR-TDB (L. Dominquez)
	Commander, U.S. Army Scientific and Technical Information Team, Europe, Box 48, APO New York 09079-4734
1	ATTN: AMXMI-E-CO
	Commander, Headquarters, 3d Ordnance Battalion, APO New York 09189-2737
1	ATTN: AEUSA-UH
	Commander, U.S. Military Academy, Department of Physics, West Point, NY 10996-1790
1	ATTN: MAJ Decker
	Headquarters, Wright Patterson Air Force Base, OH 45433-6503
1	ATTN: AFWAL/FIEEC
1	ASD/AESD
1	AAMRL/HET
1	FTD-TQTR, Wright Patterson Air Force Base, OH 45433

No. of Copies	To
1	AFWAL/FIES/SURVIAC, Wright Patterson Air Force Base, OH 45433-6553
1	AAMRL/TID, Wright Patterson Air Force Base, OH 45433-6573
	Commandant, U.S. Army Field Artillery School, Fort Sill, OK 73503-5600
1	ATTN: ATSF-GA
	Commander, Naval Air Development Center, Warminster, PA 18974-5000
1	ATTN: Code 60332 (D. Herbert)
	Commandant, U.S. Army Academy of Health Sciences, Fort Sam Houston, TX 78234-6100
1	ATTN: HSHA-CDH (Dr. R. H. Mosebar)
1	HSHA-CDS (CPT Eng)
1	HSHA-IPM
	Headquarters, Brooks Air Force Base, TX 78235-5000
1	ATTN: HSD/RDTK
1	HSD/RDS
1	USAFSAM/VNC
	Commander, U.S. Army Dugway Proving Ground, Dugway, UT 84022-5010
1	ATTN: STEDP-SO (Dr. L. Salomon)
	Commander, U.S. Army Dugway Proving Ground, Dugway, UT 84022-6630
1	ATTN: STEDP-SD-TA-F (Technical Library)
	HQ, Ogden Air Material Area, Hill Air Force Base, UT 84056-5609
1	ATTN: MMWM
	Director, U.S. Army Communications-Electronics Command, Night Vision and Electro-Optics Directorate, Fort Belvoir, VA 22060-5677
1	ATTN: AMSEL-NV-O (Dr. R. Buser)
	Commander, Marine Corps Development and Education Command, Quantico, VA 22134-5080
1	ATTN: Code D091, SPWT Section
	Deputy Director, Marine Corps Institute, Arlington, VA 22222-0001
1	ATTN: NBC CO; CO02
	Commander, U.S. Army Nuclear and Chemical Agency, 7500 Backlick Road, Bldg. 2073, Springfield, VA 22150-3198
1	ATTN: MONA-CM
	Chief of Naval Research, 800 N. Quincy Street, Arlington, VA 22217
1	ATTN: Code 441
	Commander, U.S. Army Materiel Command, 5001 Eisenhower Avenue, Alexandria, VA 22333-0001
1	ATTN: AMCCN
1	AMCSF-C
1	AMCLD
	Commander, Defense Technical Information Center, Cameron Station, Bldg. 5, 5010 Duke Street, Alexandria, VA 22304-1145
2	ATTN: DTIC-FDAC
	Commander, Naval Surface Weapons Center, Dahlgren, VA 22448
1	ATTN: Code E4311
1	Code G51 (Brumfield)

No. of Copies	To
	Commander, U.S. Army Foreign Science and Technology Center 220 Seventh Street, NE, Charlottesville, VA 22901-5396
1	ATTN: AIAST-CW2
	Director, Aviation Applied Technology Directorate, Fort Eustis, VA 23604-5577
1	ATTN: SAVRT-ATL-ASV
	Commander, U.S. Army Training and Doctrine Command, Fort Monroe, VA 23651-5000
1	ATTN: ATCD-N
1	HQ TAC/DRPS, Langley Air Force Base, VA 23665-5001
	Commander, U.S. Army Logistics Center, Fort Lee, VA 23801-6000
1	ATTN: ATCL-MGF
	Commander, U.S. Air Force Wright Aeronautical Labs, Wright-Patterson Air Force Base, OH 45433
1	ATTN: Dr. H. Graham
1	Dr. R. Ruh
1	AFWAL/MLLP, Mr. D. Forney
1	AFSC/MLLM, Dr. A. Katz
1	Aero Propulsion Labs, Mr. R. Marsh
	AVCO Corporation, Applied Technology Division, Lowell Industrial Park, Lowell, MA 01887
1	ATTN: Dr. T. Vasilos
	Materials Research Laboratories, P.O. Box 50, Ascot Vale, VIC 3032, Australia
1	ATTN: Dr. C. W. Weaver
	Case Western Reserve University, Macromolecular Science Department, Cleveland, Ohio 44106
1	ATTN: Dr. J. Koenig
	Southern Research Institute, 2000 Ninth Avenue South, Birmingham, AL 35255
1	ATTN: R. B. Spafford
	PDA Engineering, 3754 Hawkins NE, Albuquerque, NM 87109
1	ATTN: R. E. Allred
	Swedlow, Inc., 12122 Western Avenue, Garden Grove, CA 92641
1	ATTN: M. W. Preus
	Strainoptics Technologies, Inc., 108 W. Montgomery Avenue, North Wales, PA 19454
1	ATTN: A. S. Redner
	Polysar Inc., Plastics Division, P.O. Box 90, 29 Fuller Street, Leominster, MA 01453
1	ATTN: P. R. Cowley
	Loral Systems Group, P.O. Box 85, Litchfield, AZ 85340
1	ATTN: J. Uram
	McDonnell Aircraft, P.O. Box 516, St. Louis, MO 63166
1	ATTN: Mr. J. Meador, Dept. 357
	Director, U.S. Army Materials Technology Laboratory, Watertown, MA 02172-0001
2	ATTN: SLCMT-TML
2	Authors

U.S. Army Materials Technology Laboratory,
Watertown, Massachusetts 02172-0001
SOLVENT ASSISTED DELAMINATION CRACK GROWTH BEHAVIOR OF AMORPHOUS THERMOPLASTIC MATERIALS
Janice J. Vanselow and Alex J. Hsieh

Technical Report MTL TR 89-17, February 1989, 14 pp - illustrations, AMCMS Code 612105.H840011

AD________________

UNCLASSIFIED
UNLIMITED DISTRIBUTION

Key Words

Environmental tests
Amorphous materials
Composite materials

Crack growth studies are being carried out with o-xylene in an amorphous thermoplastic, polyetherimide (PEI), via a static deadweight loading apparatus. The three systems evaluated were the neat resin, composite, and adhesively bonded composite. The neat resin specimens show striationlike crack growth band markings on the fracture surfaces. The spacing between the growth bands increases with increasing crack length in each specimen. In the case of the adhesively bonded composite, a characteristic mosaic pattern of intersecting cracks normal to the plane of the adhesive was seen on the fracture surfaces. These cracks, as well as matrix cracks perpendicular to the fibers seen on the fractured composite specimens, appear to result from residual stress driven solvent cracking. Although the rates of crack propagation in the composite systems are much slower than those in the neat resin at most G_I values, the mode of solvent-induced degradation is shown to be matrix dominated.

U.S. Army Materials Technology Laboratory,
Watertown, Massachusetts 02172-0001
SOLVENT ASSISTED DELAMINATION CRACK GROWTH BEHAVIOR OF AMORPHOUS THERMOPLASTIC MATERIALS
Janice J. Vanselow and Alex J. Hsieh

Technical Report MTL TR 89-17, February 1989, 14 pp - illustrations, AMCMS Code 612105.H840011

AD________________

UNCLASSIFIED
UNLIMITED DISTRIBUTION

Key Words

Environmental tests
Amorphous materials
Composite materials

Crack growth studies are being carried out with o-xylene in an amorphous thermoplastic, polyetherimide (PEI), via a static deadweight loading apparatus. The three systems evaluated were the neat resin, composite, and adhesively bonded composite. The neat resin specimens show striationlike crack growth band markings on the fracture surfaces. The spacing between the growth bands increases with increasing crack length in each specimen. In the case of the adhesively bonded composite, a characteristic mosaic pattern of intersecting cracks normal to the plane of the adhesive was seen on the fracture surfaces. These cracks, as well as matrix cracks perpendicular to the fibers seen on the fractured composite specimens, appear to result from residual stress driven solvent cracking. Although the rates of crack propagation in the composite systems are much slower than those in the neat resin at most G_I values, the mode of solvent-induced degradation is shown to be matrix dominated.

U.S. Army Materials Technology Laboratory,
Watertown, Massachusetts 02172-0001
SOLVENT ASSISTED DELAMINATION CRACK GROWTH BEHAVIOR OF AMORPHOUS THERMOPLASTIC MATERIALS
Janice J. Vanselow and Alex J. Hsieh

Technical Report MTL TR 89-17, February 1989, 14 pp - illustrations, AMCMS Code 612105.H840011

AD________________

UNCLASSIFIED
UNLIMITED DISTRIBUTION

Key Words

Environmental tests
Amorphous materials
Composite materials

Crack growth studies are being carried out with o-xylene in an amorphous thermoplastic, polyetherimide (PEI), via a static deadweight loading apparatus. The three systems evaluated were the neat resin, composite, and adhesively bonded composite. The neat resin specimens show striationlike crack growth band markings on the fracture surfaces. The spacing between the growth bands increases with increasing crack length in each specimen. In the case of the adhesively bonded composite, a characteristic mosaic pattern of intersecting cracks normal to the plane of the adhesive was seen on the fracture surfaces. These cracks, as well as matrix cracks perpendicular to the fibers seen on the fractured composite specimens, appear to result from residual stress driven solvent cracking. Although the rates of crack propagation in the composite systems are much slower than those in the neat resin at most G_I values, the mode of solvent-induced degradation is shown to be matrix dominated.

U.S. Army Materials Technology Laboratory,
Watertown, Massachusetts 02172-0001
SOLVENT ASSISTED DELAMINATION CRACK GROWTH BEHAVIOR OF AMORPHOUS THERMOPLASTIC MATERIALS
Janice J. Vanselow and Alex J. Hsieh

Technical Report MTL TR 89-17, February 1989, 14 pp - illustrations, AMCMS Code 612105.H840011

AD________________

UNCLASSIFIED
UNLIMITED DISTRIBUTION

Key Words

Environmental tests
Amorphous materials
Composite materials

Crack growth studies are being carried out with o-xylene in an amorphous thermoplastic, polyetherimide (PEI), via a static deadweight loading apparatus. The three systems evaluated were the neat resin, composite, and adhesively bonded composite. The neat resin specimens show striationlike crack growth band markings on the fracture surfaces. The spacing between the growth bands increases with increasing crack length in each specimen. In the case of the adhesively bonded composite, a characteristic mosaic pattern of intersecting cracks normal to the plane of the adhesive was seen on the fracture surfaces. These cracks, as well as matrix cracks perpendicular to the fibers seen on the fractured composite specimens, appear to result from residual stress driven solvent cracking. Although the rates of crack propagation in the composite systems are much slower than those in the neat resin at most G_I values, the mode of solvent-induced degradation is shown to be matrix dominated.